THE AMERICAN MINERALOGIST, VOL. 52, JANUARY–FEBRUARY, 1967

INFRARED STUDIES OF THE VARIATION OF H-BONDED OH IN SYNTHETIC α-QUARTZ[1]

D. M. Dodd and D. B. Fraser, *Bell Telephone Laboratories, Incorporated, Murray Hill, New Jersey.*

Abstract

The extinction coefficient at 3500 cm^{-1} (α_{3500}) near the maximum of the broad background absorption band in the spectrum of α-quartz is proportional to the H-bonded OH content. At this frequency and at a crystal temperature of $\sim$300°K, infrared measurements were made on several thin Y-cut samples. In each case, the radiation beam was parallel to Y[10.0] and the sample was translated across the beam in the Z direction [00.1]. The resulting maps of the variations of α_{3500} show that the H-bonded OH content of the cultured material is not related to that of the seed. Each α_{3500} topograph is fairly symmetrical about the parallel to the X-axis centerline implying a relationship between H-bonded OH content and growth rate. In one sample, the growth rate was purposely accelerated at about the halfway point. This change in growth rate caused an increase in α_{3500} (H-bonded OH content).

Synthetic crystalline α-quartz often exhibits lamellar inhomogeneities or striations which, in the Z-growth region, are approximately parallel to the (00.1) plane. Comparisons of α_{3500} topographs with Schlieren photographs of untreated and heat-treated samples and with Twyman-Green interferograms for the same set of specimens indicate the following:

(1) Changes in growth rate cause striations.
(2) Milky layers (inclusions of ordered water), seen in some samples after prolonged heat treatment at $T \geq 500$°C, develop in regions of originally higher α_{3500} (H-bonded OH content) which are also those of initially lower refractive index.
(3) There is a one to one correspondence between the α_{3500} (H-bonded OH content) variations, the striation boundaries, and the refractive index gradients.

Introduction

Homogeneous α-quartz (low-quartz) is required for various optical and acoustic components, but the synthetic material often exhibits objectional lamellar inhomogenieties sometimes called striations (Arnold, 1956; 1957) or "growth lines." These features and the seed in the center of the sample can be seen in Figure 1 which is a Schlieren photograph (taken in collimated light) of a thin (0.300 cm) Y-cut slice of synthetic quartz crystal #102. In the Z-growth regions on either side of the seed, the striations are approximately parallel to the (00.1) or basal plane.

The broad background absorption band with its maximum near 3500 cm^{-1} in the spectrum of α-quartz is due to H-bonded OH (Brunner, *et al*, 1961; Kats, 1962; Dodd and Fraser, 1965) and the extinction coefficient at this frequency (α_{3500} = absorbance ÷ sample thickness, d, in cm) is related to anelastic loss (Dodd and Fraser, 1965) as well as being proportional to H-bonded OH content. From Hetherington's and Jack's

---

[1] Includes most of the material presented at 8th European Congress on Molecular Spectroscopy, Copenhagen, Denmark, August 14–20, 1965.

(1962) figures for fused silica which are in rough agreement with those of Scholze (1960), Bambauer (1961), and Brunner *et al* (1961) for crystalline α-quartz,

$$\text{wt \% H-bonded OH} = 0.01\ \alpha_{3500}.$$

Furthermore, a 0.001 wt. % increase in OH corresponds to a decrease in the refractive index of vitreous silica of 1×10^{-6} (Hetherington and Jack, 1962) and the same may be true for crystalline α-quartz.

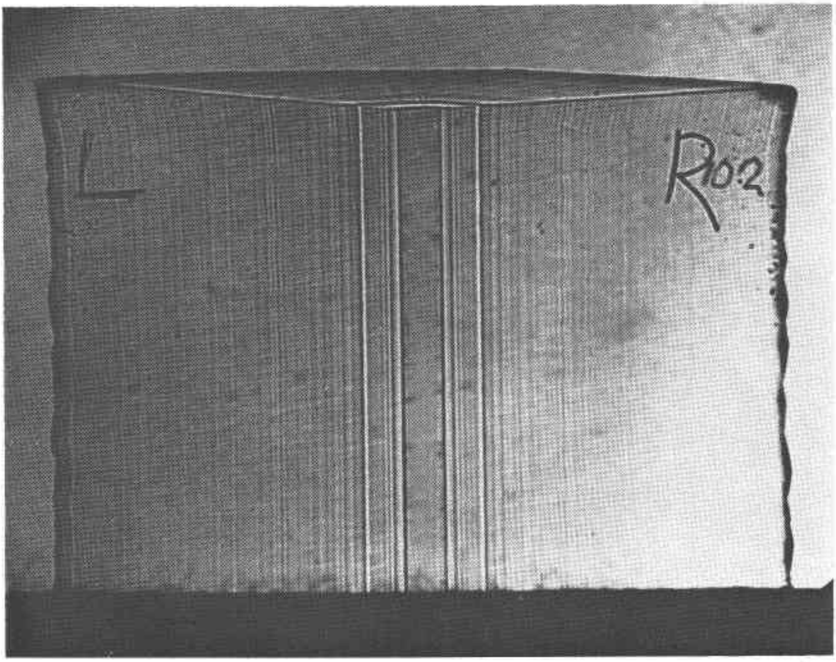

FIG. 1. Schlieren photograph of Synthetic quartz Crystal #102.

In the hope of discovering the nature and cause of the striations, it was decided to map for a series of Y-cut samples (a) the α_{3500} values across the faces parallel to (10.0) as a means of ascertaining the corresponding changes in H-bonded OH content and to study (b) the refractive index variations in order to see if a correlation exists between (a) and (b), the striations, and growth rate variations in the autoclave.

EXPERIMENTAL

The samples investigated were Y-cut slices of synthetic α-quartz with plane polished faces parallel to (10.0). Each crystal was grown by the

TABLE I. Y-CUT SYNTHETIC QUARTZ SAMPLE DESCRIPTIONS

Sample Designation	d(cm)	Solution	Fill(%)	BT(°F)[1]	ΔT(°F)[2]	Pressure (psi)	Growth Rate[3] (mils/da)
27	0.215	2.5*M* NaOH 1.0*M* KOH Fe doped (from autoclave)	82	748	98	?	41
86	0.238	0.5*M* NaOH 0.05*M* $LiBO_2$	83	695	80	17,500	45
102	0.300	0.05*M* NaOH 0.05*N* Li_2CO_3	82	680	73	19,000	36.3
115	0.312	1.0*M* NaOH 0.1*M* $LiBO_2$	82	710	55	?	47
				for 13 days and then			
				755	100	?	62
				for 9 days			
125	0.299	1.0*M* NaOH 0.1*M* $LiBO_2$	82	715	55	23,000	38
126	0.295	1.0*M* NaOH 0.015*M* Al 0.004*M* Co	82	745	80	25,500	65

[1] BT = Temperature at bottom of autoclave.

[2] ΔT = Temperature gradient in autoclave (bottom to top).

[3] Growth rate in direction 5° off Z.

Western Electric Company on a synthetic seed cut 5° off the basal plane and with the long dimension parallel to the Y-axis. Further descriptions are in Table I.

A Model 12G Perkin-Elmer Spectrometer equipped with KBr fore-prism, 300 lines/in. grating, and Leeds and Northrup recorder was used for the infrared mapping measurements. The entrance port was reduced in height by a factor of ~0.5 and the grating monochromator slits were made as narrow as feasible to permit measurements on minimal sample cross-sections (~2.6×0.5 mm). The commercial source unit was replaced by a custom-made one as shown in Figure 2. Each *Y*-cut sample, positioned with *Z*-axis horizontal and with polished faces perpendicular to the radiation at the source image, was held in a vertically mounted mechanical microscope stage which was graduated in millimeters. During the course of measurement, a 12 RPH motor, coupled to the stage, moved the sample slowly (2.6 mm/min) and uniformly across the radiation beam.

Refractive index studies and measurements were made on a Twyman-Green interferometer.

RESULTS AND DISCUSSION

Figure 3 shows, in order from top to bottom, the trace obtained at 3900 cm^{-1} with no sample in the light path, the map for synthetic quartz crystal #86 at 3900 cm^{-1} where there are no absorption bands, and the α_{3500} topograph for the same crystal. The first shows the instrumental variation during the course of a run while the second, taken as the zero absorbance line for α-quartz and thereby correcting for reflection losses, indicates that the fluctuations in the α_{3500} topograph and in subsequent spectral maps at 3500 cm^{-1} are actually variations in extinction coefficient caused by corresponding changes in H-bonded OH content and are not a result of reflectance differences associated with refractive index variations.

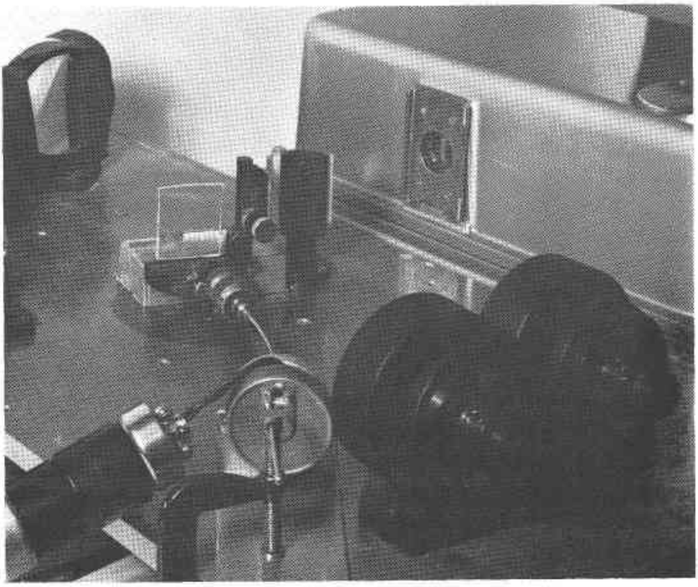

FIG. 2. Custom-made source unit for Model 12G Perkin-Elmer spectrometer. Sample, at focal point, is held in vertically-mounted mechanical microscope stage coupled to 12 RPH motor.

The topographical survey for synthetic quartz crystal #102 (Fig. 4) pictures the α_{3500} (H-bonded OH) variations determined by six scans

(A) parallel to the Z-axis at several positions along the X-axis and one scan (B) along a line in the X direction. The shaded rectangles, drawn to scale, represent the sampling areas in the two respective orientations. It is seen that the six traces (A) are almost superposable. This should be the case if the striations, parallel to the X-axis, are regions of change in H-bonded OH content.

Figures 5–10 present α_{3500} maps for various synthetic quartz samples. In some cases, the seeds are all of relatively low α_{3500} value (H-bonded OH content), while in others the 3500 cm^{-1} extinction coefficient (H-bonded OH content) of the seed is comparatively high. Apparently, the quality of synthetic quartz is not determined by the H-bonded OH content of the seed. It is evident, too, that each α_{3500} topograph is nearly symmetrical about the center line parallel to the X-axis and corresponding to the middle of the seed. This is to be expected if the variations of α_{3500} (H-bonded OH content) are associated with fluctuations in growth rate since growth takes place equally on either side of the seed.

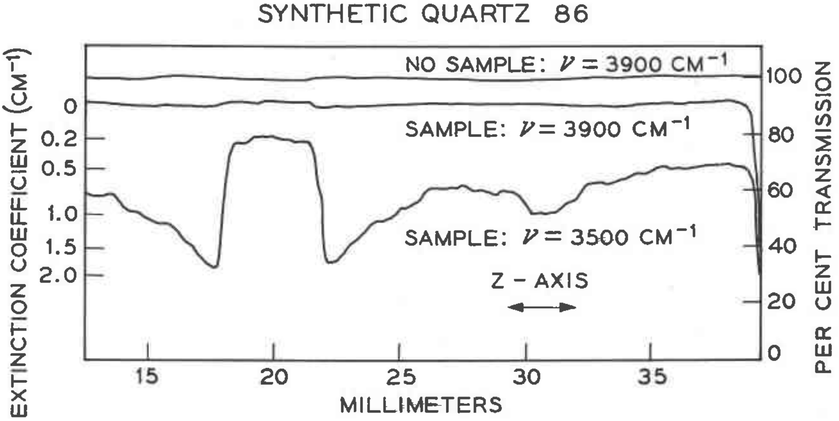

FIG. 3. Synthetic quartz crystal #86: Top trace: Scan at 3900 cm^{-1} with no sample in beam. Middle trace: Scan at 3900 cm^{-1} with sample in beam. Bottom trace: Scan at 3500 cm^{-1} with sample in beam, α_{3500} topograph.

Figure 8 shows not only (B) the α_{3500} map for synthetic quartz #86, but also (A) a strip of its photograph taken in collimated light and (C) a strip of the Twyman-Green interferogram. These items have been so aligned that it can readily be seen that there is a one to one correspondence between the striations, the variations in refractive index, and the changes in α_{3500} (H-bonded OH content). Furthermore, there is indeed an inverse relationship between refractive index and α_{3500} (H-bonded OH content).

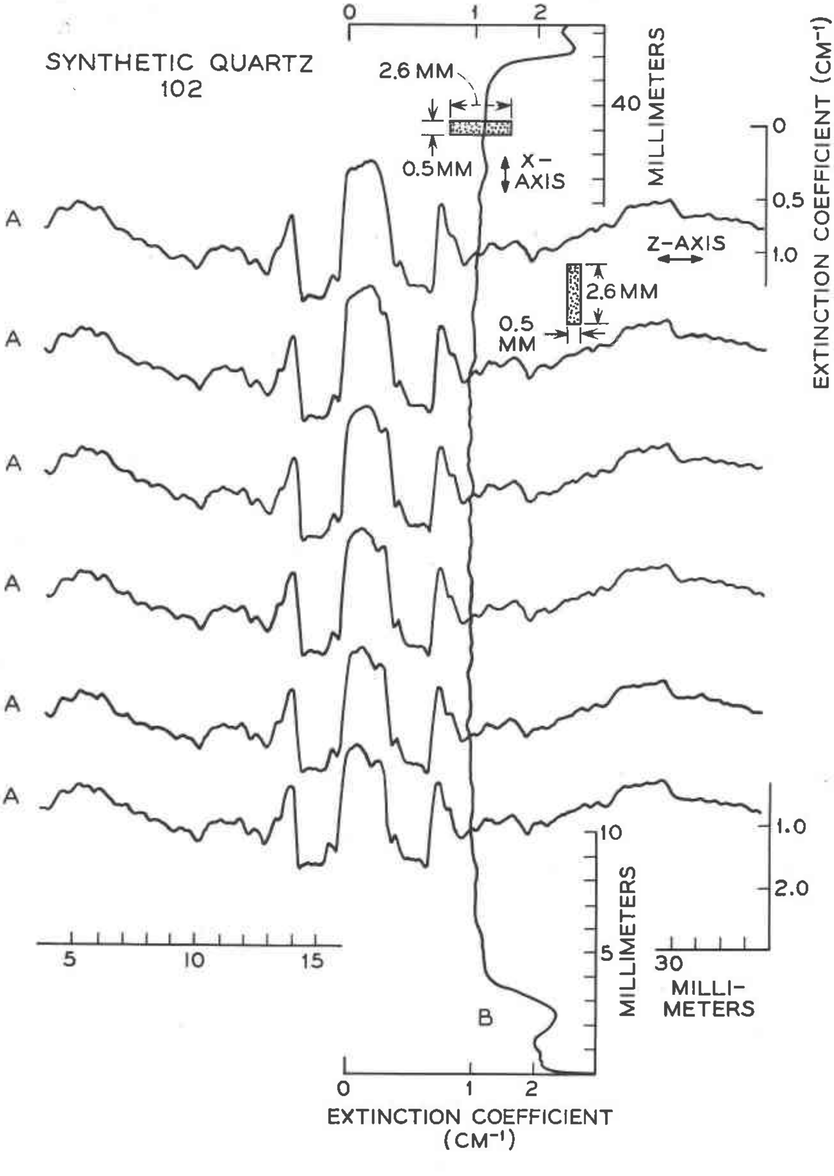

FIG. 4. Topographical α_{3500} survey for synthetic quartz crystal #102.

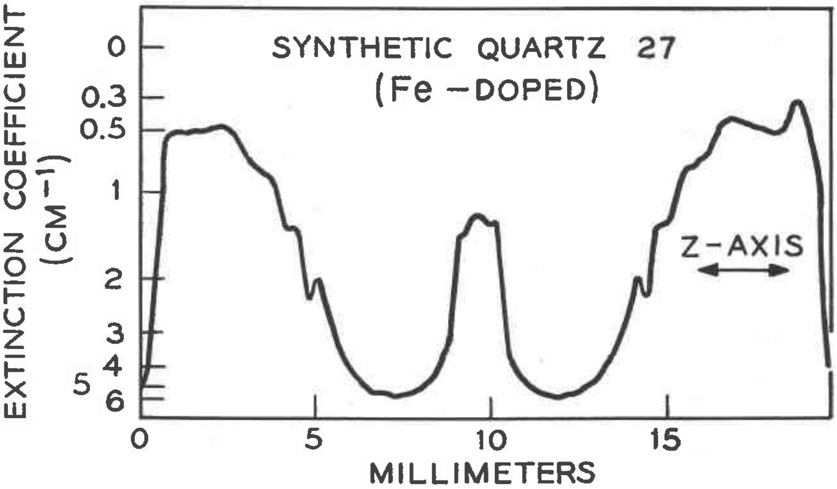

FIG. 5. α_{3500} topograph for synthetic quartz crystal #27.

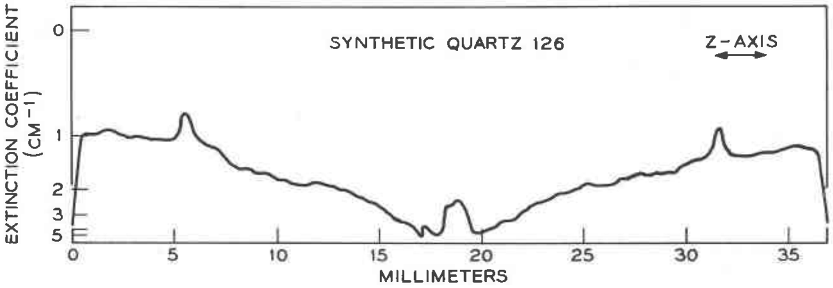

FIG. 6. α_{3500} topograph for synthetic quartz crystal #126.

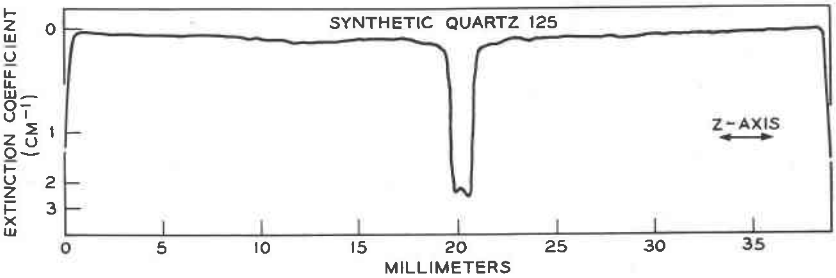

FIG. 7. α_{3500} topograph for synthetic quartz crystal #125.

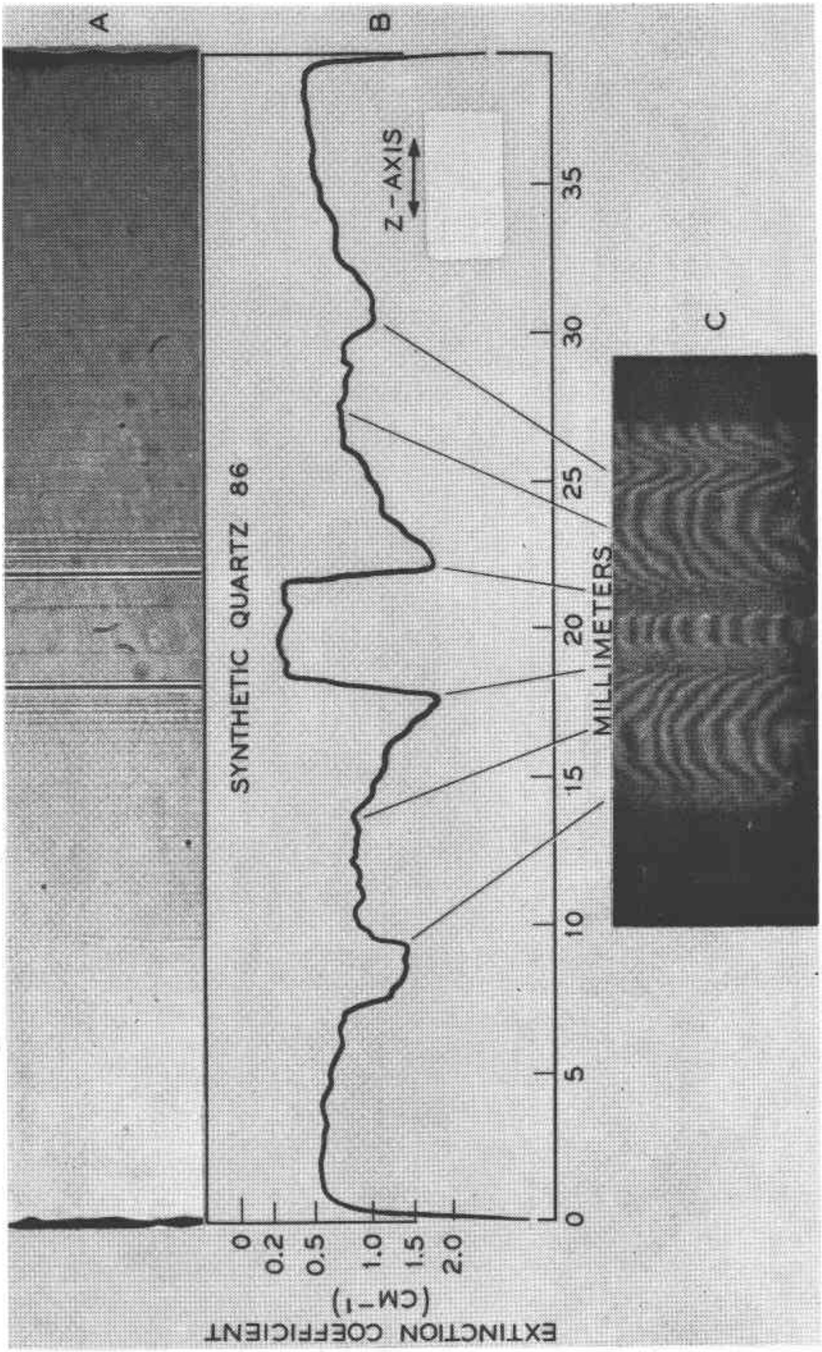

FIG. 8. Synthetic quartz crystal #86: A: Schlieren photograph; B: α_{3500} topograph; C: Twyman-Green interferogram.

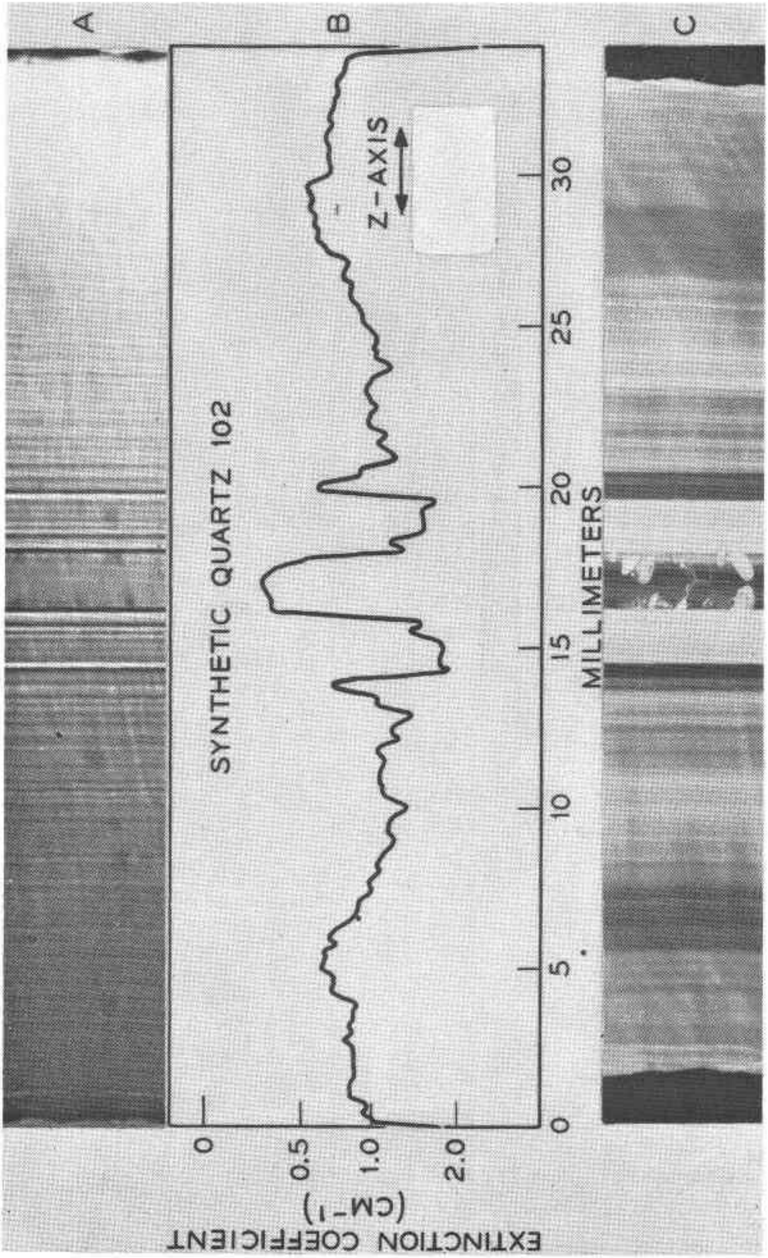

FIG. 9. Synthetic quartz crystal #102; A: Schlieren photograph; B: α_{3500} topograph; C: Photograph of sample after baking at $T \geq 500$°C.

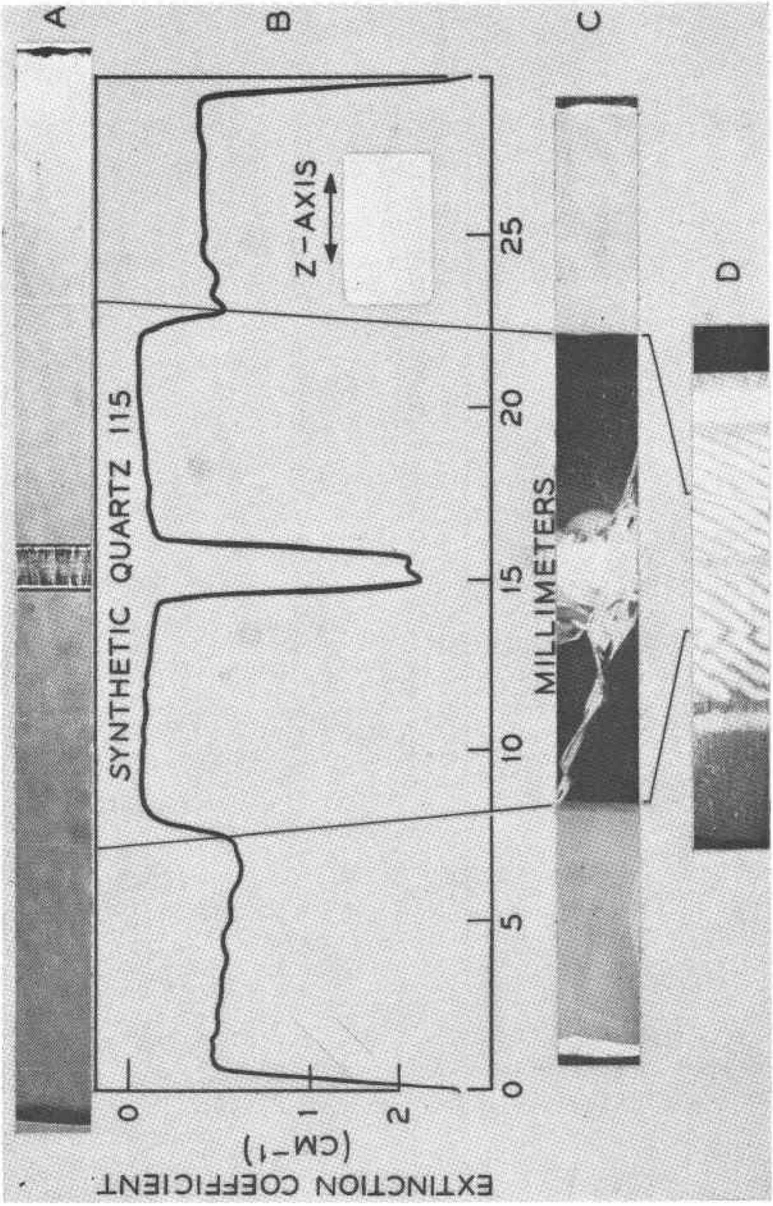

FIG. 10. Synthetic quartz crystal #115: A: Schlieren photograph; B: α_{3500} topograph; C: Photograph of sample after baking at $T \geq 500$°C; D: Twyman-Green interferogram.

After prolonged baking in air at $T \geq 500°C$, some synthetic quartz specimens become milky in layers parallel to the seed plate (Dodd and Fraser, 1965; Cohen and Hodge, 1958). These bands have been found to contain ordered water (Dodd and Fraser, 1965). Figure 9 shows, for synthetic quartz crystal #102, the alignment of (A) a strip of the photograph taken in collimated light, (B) the α_{3500} topograph, and (C) a strip of the photograph of the sample after baking. Here we see one to one correspondence between the striations, the α_{3500} topographical features (H-bonded OH content), and the milky bands. It is evident that the milky layers, as reported heretofore (Dodd and Fraser, 1965), are regions which originally exhibited greater α_{3500} values (H-bonded OH content).

Synthetic quartz crystal #115 was slowly grown for a time and then the growth rate was accelerated. (See Table 1.) For 13 days, this sample grew at the rate of 47 mils per day which means that, measured in the Z direction, its total length at the time of growth rate acceleration was 610 mils or 16 mm. Two fairly large increases in α_{3500} (H-bonded OH content) occur (Fig. 10, B), one at about the 7 mm and the other at about the 23 mm point. Since these features are 16 mm apart, they must have been caused by the change in growth rate. It will be noted that each corresponds to a sizable striation in the sample (Fig. 10, A), to the inner edge of a milky region (Fig. 10, C), and to a decrease in refractive index (Fig. 10, D). Figure 10, therefore, provides additional and very convincing proof that the striations are caused by growth rate variations and are regions of change in H-bonded OH content and in refractive index.

CONCLUSIONS

The α_{3500} topographs indicate that the quality of cultured quartz is not dependent upon that of the seed and the topographical symmetry implies a relationship between growth rate and variations in H-bonded OH content. In addition, a one to one correspondence exists between the striations, the variations in refractive index, and the changes in α_{3500} (H-bonded OH content). The striations have been found to be associated with the milky layers produced by drastic heating. These layers are known to contain inclusions of ordered water and to form in regions where, before heat treatment, α_{3500} (H-bonded OH content) was relatively larger. Furthermore, study of a sample in which the growth rate was purposely increased confirms the fact that this change in growth rate causes a pair of striations one on either side of the seed. Each corresponds to an increase in H-bonded OH content, to the beginning of a milky zone, and to a decrease in refractive index.

ACKNOWLEDGMENTS

The authors wish to thank K. H. Storks and D. L. Wood for many helpful suggestions, D. W. Rudd and N. Lias (Western Electric Company) as well as A. A. Ballman for supplying the crystals, D. R. Herriott and J. R. Wimperis for the use of the Twyman-Green interferometer, and S. S. DeBala for technical assistance.

REFERENCES

ARNOLD G. W., JR., (1956) Defects in quartz crystals. *Ann. Symp. Frequency Contr., Ft. Monmouth, N. J., 10th, Proc.*, p. 61–74

——— (1957) Defects in quartz crystals. *Ann. Symp. Frequency Contr., Ft. Monmouth, N.J., 11th, Proc.*, p. 112–129.

BAMBAUER, H. U. (1961) Spurenelementgehalte und γ-Farbzentren in Quarzen aus Zerrklüften der Schweizer Alpen. *Schweiz. Mineral. Petrogr. Mitt.* **41,** 335–369.

BRUNNER, G. O., H. WONDRATSCHEK, AND F. LAVES (1961) Ultrarotuntersuchungen über den Einbau von H in natürlichen Quartz. *Z. Elektrochem.* **65,** 735–750.

COHEN, A. J. AND E. S. HODGE (1958) Zonal specificity and nonspecificity of certain impurities during growth of synthetic α-quartz. *J. Phys. Chem. Solids* **7,** 361–362.

DODD, D. M. AND D. B. FRASER (1965) The 3000–3900 cm^{-1} absorption bands and anelasticity in crystalline α-quartz. *J. Phys. Chem. Solids,* **26,** 673–686.

HETHERINGTON, G. AND K. H. JACK (1962) Water in vitreous silica. I. Influence of "water" content on the properties of vitreous silica. *Phys. Chem. Glasses* **3** (4), 129–133.

KATS, A. (1962) Hydrogen in alpha-quartz. *Philips Res. Rep.* **17,** 133–195 and 201–279.

SCHOLZE, H. (1960) Über die quantitative UR-spektroskopie Wasserbestimmung in Silikaten. *Fortschr. Mineral.* **38,** 122–123.

Manuscript received, April 18, 1966; accepted for publication, May 16, 1966.